Geomorphology 101 (2008) 631–642

Contents lists available at ScienceDirect

Geomorphology

journal homepage: www.elsevier.com/locate/geomorph

GIS-based landslide susceptibility mapping for the 2005 Kashmir earthquake region

Ulrich Kamp [a,*], Benjamin J. Growley [a], Ghazanfar A. Khattak [b], Lewis A. Owen [b]

[a] Department of Geography, The University of Montana, Missoula, MT 59812, USA
[b] Department of Geology, University of Cincinnati, Cincinnati, OH 45221, USA

ARTICLE INFO

Article history:
Received 21 September 2007
Received in revised form 1 March 2008
Accepted 3 March 2008
Available online 14 March 2008

Keywords:
Earthquake
GIS
Hazard
Himalaya
Landslides
Susceptibility

ABSTRACT

The M_w 7.6 October 8, 2005 Kashmir earthquake triggered several thousand landslides throughout the Himalaya of northern Pakistan and India. These were concentrated in six different geomorphic–geologic–anthropogenic settings. A spatial database, which included 2252 landslides, was developed and analyzed using ASTER satellite imagery and geographical information system (GIS) technology. A multi-criterion evaluation was applied to determine the significance of event-controlling parameters in triggering the landslides. The parameters included lithology, faults, slope gradient, slope aspect, elevation, land cover, rivers and roads. The results showed four classes of landslide susceptibility. Furthermore, they indicated that lithology had the strongest influence on landsliding, particularly when the rock is highly fractured, such as in shale, slate, clastic sediments, and limestone and dolomite. Moreover, the proximity of the landslides to faults, rivers, and roads was also an important factor in helping to initiate failures. In addition, landslides occurred particularly in moderate elevations on south facing slopes. Shrub land, grassland, and also agricultural land were highly susceptible to failures, while forested slopes had few landslides. One-third of the study area was highly or very highly susceptible to future landsliding and requires immediate mitigation action. The rest of the region had a low or moderate susceptibility to landsliding and remains relatively stable. This study supports the view that (1) earthquake-triggered landslides are concentrated in specific zones associated with event-controlling parameters; and (2) in the western Himalaya deforestation and road construction contributed significantly to landsliding during and shortly after earthquakes.

1. Introduction

On October 8, 2005 at 8:50:40 am local time (03:50:40 UTC) a devastating earthquake with the moment magnitude of 7.6 struck the Lesser Himalaya of northern Pakistan and India. The earthquake's epicenter was located at 34°29′35″N and 73°37′44″E at a depth of 26 km, ~10 km northeast of the city of Muzaffarabad, the regional capital of Azad Kashmir (Fig. 1). During the following 19 days, 978 aftershocks of magnitudes ≥4.0 shook the region (EERI, 2005). The earthquake is the deadliest in recent history of the Indian subcontinent, with >86,000 fatalities, >69,00 injuries and >32,000 buildings destroyed displacing ~2.8 million people in Pakistan (Peiris et al., 2006; USGS, 2006). In India, >1300 people were killed, >6000 were injured, and many buildings were extensively damaged (Vinod Kumar et al., 2006). The loss of life is mainly attributed to collapsing structures due to poor building materials and architectural design. The devastation was exasperated by the many thousands of mass movements that were triggered by the earthquake, which resulted in ~1000 direct fatalities and many more indirectly due to the disruption of communication links.

Landsliding is one of the most prevalent hazards in the Himalaya and can be particularly devastating when it occurs adjacent to human settlements and infrastructures, such as towns, roads, bridges and utilities. Landsliding is common in the Himalaya because of the active seismicity, great relief, heavy monsoon rains, and accelerated erosion due to deforestation and construction. In the wake of this recent disaster, it is ever more apparent that new standards in home and road construction, and planning based on geomorphic and tectonic data are needed to help mitigate future disasters. For effective landslide hazard reduction the analysis of slope failures requires a comprehensive analysis of the landscape using modern technologies and data exchange to ensure that the proper procedures and policies are put into effect in a timely fashion (Saha and Gupta, 2002).

The first step of any landslide damage assessment and management is a landslide inventory map providing the locations and outlines of landslides and, in the case of larger scale maps, also the classification of landslides types (Spiker and Gori, 2000; Chacon et al., 2006). The second step requires the production of a landslide susceptibility map, which includes the spatial distribution of event-controlling parameters, such as, lithology and slope gradient that are responsible for slope failures. This will allow landslide-prone areas to be defined, independent of temporal controls, and indicate where landslides may likely occur in the future (Chacon et al., 2006). The third step is the production of a landslide hazard map, which, in

* Corresponding author.
E-mail address: ulrich.kamp@umontana.edu (U. Kamp).

0169-555X/$ – see front matter © 2008 Elsevier B.V. All rights reserved.
doi:10.1016/j.geomorph.2008.03.003

contrast to landslide susceptibility mapping, includes a temporal framework, with the probability of landslide occurrence within a specified period of time. This ranks different parts of the study area on the basis of the degree of the actual or potential hazard from landslides (Varnes, 1984). The final step involves the creation of a landslide risk map, which describes the expected annual cost of landslide damage throughout the affected area (Spiker and Gori, 2000; Espizua and Bengochea, 2002; Remondo et al., 2008; Zêzere et al., 2008). Developing a risk map requires a multidimensional perspective; therefore, in the future, the innovative studies of landslide risk will be those that combine, in a creative manner, the work of both physical and social scientists (Alexander, 2008). Ultimately all four maps are used to delimit and present of zones of landslide susceptibility, hazard and risk, respectively. A landslide zone is essentially a division of the land into areas and their classification according to degrees of actual or potential landslide hazard or susceptibility (Van Westin et al., 2003).

The terms landslide susceptibility map and landslide hazard map are often used interchangeable. A natural hazard, *senso stricto*, however, involves a threat to the life of human and/or their animals, actual casualties and/or fatalities, and property (building and land) damage (Alexander, 2005; Abbott, 2007). Therefore, areas that are susceptible to landslides, but do not affect humans can not be considered as hazardous. Strictly speaking, most landslide hazard maps should really be considered as landslide susceptibility maps as they often do not fully consider the human dimension (Brabb, 1984). With increased population pressure and expansion into marginal regions, landslide susceptibility/hazard/risk mapping is a rapidly advancing field, but few studies have been undertaken in the Himalaya (e.g., Anbalagan, 1992; Sharma and Kandpal, 1996; Virdi et al., 1997; Bhatnagar, 1998; Pachauri et al., 1998; Lee and Min, 2001; Dai and Lee, 2002; Joshi et al., 2003; Saha et al., 2005; Sarkar and Gupta 2005).

In response to the recent disaster in Kashmir and the need for increased awareness and methods to deal with landsliding in the Himalaya, we have undertaken a study of the landsliding in the earthquake affected region of northern Pakistan. Our study presents a map of susceptibility to future landsliding for the region, which is centered on the epicenter of the 2005 Kashmir earthquake. We believe this study will aid in planning appropriate quick and safe mitigation measures and future development strategies based on the identification of landslide-prone areas within the region. Our study provides a model that may be applied to other regions of the Himalaya and high mountains elsewhere in the world.

2. Study area

The study area is located in the state of Azad Jammu and Kashmir in the Lesser Himalaya of northern Pakistan and was centered on the earthquake's epicenter enclosing an area of ~2550 km^2 with a

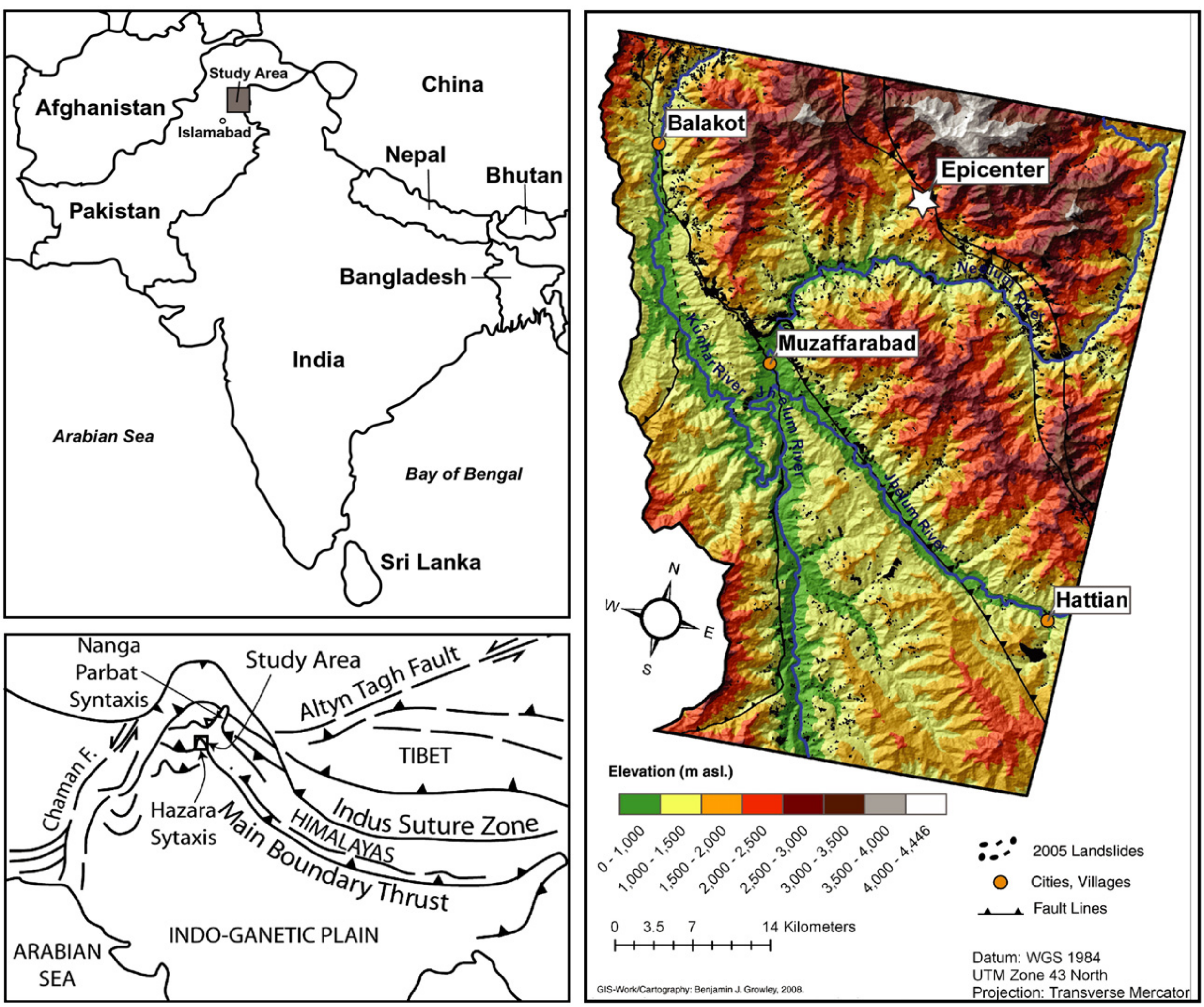

Fig. 1. The study area of the 2005 Kashmir earthquake in northern Pakistan. The epicenter lies ~10 km northeast of Muzaffarabad, the district capital of the state of Azad Jammu and Kashmir in northern Pakistan. (The color version of this figure is available in the web version of this article.)

perimeter of ~228 km (Fig. 1). The district capital Muzaffarabad lies only ~50 km west of the Pakistani–India Line of Control and is positioned on the confluence of the Jhelum and Neelum rivers.

Geologically the region encloses the Hazara–Kashmir Syntaxis, which is delimited by the Main Boundary Thrust (MBT) and represents a region of considerable crustal shortening and uplift (Calkins et al., 1975; Hussain and Khan, 1996; Kazmi and Jan, 1997; Hussain et al., 2004) (Fig. 2). Most of the terrain is mountainous with the highest peaks exceeding 4500 m above sea level (asl). The landscape is deeply dissected with the main valley floors between ~500 and >2000 m asl. The region is drained by the Jhelum River and its two tributaries the Neelum and Kunhar rivers. These rivers flow westward forming deep antecedent valleys before flowing southwards along broader valleys to the Indo-Gangetic Plain. These three main rivers flow very rapidly with discharges of approximately 470, 240, and 80 m^3/s, respectively (Pakistan Water Gateway, 2007). This has resulted in intense fluvial incision and resultant high erosion rates, producing steep lower valley slopes that exceed 50°. Above these lower steep valley slopes, the hill slopes become less steep (commonly 10–25°) before being replaced by the steeper (>50°) high glaciated summit slopes.

The study area has a subtropical highland climate. The mountainous terrain produces variable weather patterns. In Muzaffarabad (at ~700 m asl), the mean maximum and minimum temperatures in January are 15.9 °C and 3.2 °C and in June 37.6 °C and 22.1 °C (WMO, 2007). Muzaffarabad receives ~1500 mm precipitation on average during the year, of which one-third falls as rain during the monsoon season from late June until the end of August (District Census Report, 1998). This often results in severe flooding and landslides, notably debris flows. During the winter, precipitation falls as snow at elevations above ~1500 m asl. Little precipitation occurs in spring, but snowmelt provides abundant surface waters to slopes, which results in erosion and/or infiltration into slopes increasing the height of the groundwater table.

Population densities in northern Pakistan are extremely high, for example, Azad Jammu and Kashmir had a density of 350 people/km^2 in 2007 (World Gazetteer, 2007). The population is concentrated along the valley floors, on river terraces and on areas that have gentle slopes. The study area includes four larger urban concentrations of which Muzaffarabad (population of ~20,800 in 2007) is the largest. The high population densities place a severe environmental pressure on the mountain's ecosystems.

The rugged terrain and intense summer rainfall make transportation extremely difficult through the region. Many roads are constructed along steep slopes often by excavating deep notches into the weathered bedrock and/or on fill that is perched precariously on steep slopes. These are very unstable and landsliding is common along most highways.

3. Landslide types

Shortly after the earthquake (November 2005), Owen et al. (2008) examined 1293 landslides at 174 locations in the study area. They developed a landslide inventory and classified the landslides into six geomorphic–geologic–anthropogenic settings. These includes: (i) mainly rock falls in highly fractured carbonate rocks comprising the lowest beds in the hanging wall of the likely earthquake fault; (ii) mostly rock falls and rock slides in Tertiary siliciclastic rocks along antecedent drainages that traverse the Hazara–Kashmir Syntaxis; (iii) natural failures in high and/or

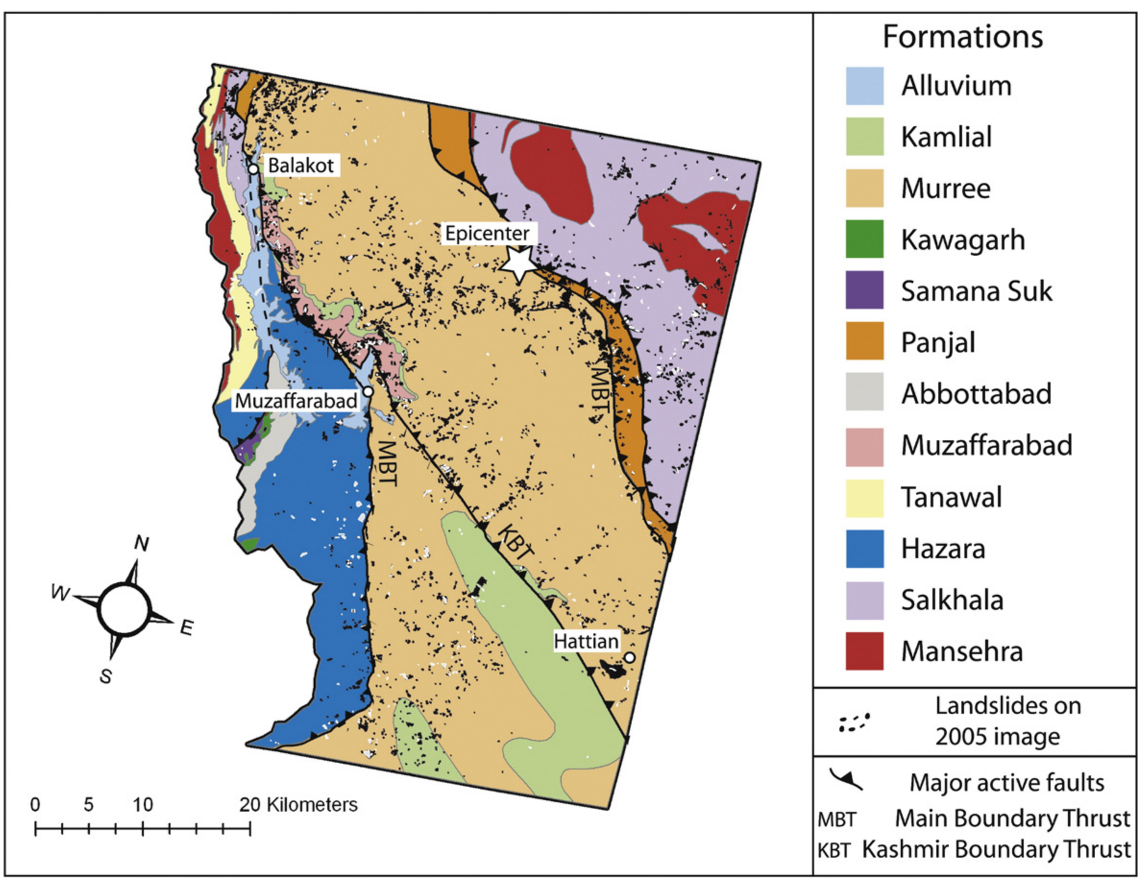

Fig. 2. Geological map of the study area of the 2005 Kashmir earthquake (compiled, digitized, and revised after maps by Hussain and Khan, 1996 and Hussain et al., 2004). Most (63%) of the landslides occurred in the Murree Formation. The Tanawal Formation has the highest landslide density (>3/km^2). The Muzaffarabad Formation has the highest (4.3%) percentage of landslide-covered area and the largest (~36,000 m^2) mean landslide size. (The color version of this figure is available in the web version of this article.)

fluvially incised steep (50–60°) slopes comprising Precambrian and Lower Paleozoic rocks; (iv) mostly small debris falls in very steep (>60°) lower slopes of fluvially undercut Quaternary valley fills; (v) many small rock falls and shallow rock slides on ridges and spur crests; and (vi) failures in locations associated with road construction that traverses steep (>50°) slopes. For our susceptibility mapping we revisited and re-photographed all locations included in the inventory by Owen et al. (2008) in May and June 2006.

Most (>90%) of the earthquake-induced landslides were rock and debris falls ranging from a few m^3 to $>10^3$ m^3 in size; but also included debris slides and debris flows (using Varnes' 1978 classification; Owen et al., 2008). Owen et al. (2008) also noted extensive fissuring in many of the valley slopes and warned of the hazard of future landsliding, particularly during or after the ensuing snowmelt season. The most extensive fissuring was associated with the Muzaffarabad Formation, comprising highly fractured Precambrian dolomites and siliclastics, along the west side of the Kaghan Valley between Muzaffarabad and Balakot.

The largest landslide, the Hattian sturzstrom, was located in a tributary of the Jhelum Valley in the Murree Formation (Harp and Crone, 2006; Owen et al., 2008). Its scar was >1 km long, >200 m wide, and >20 m deep and sloping northwards between 60–70° (Owen et al., 2008). Dunning et al. (2007) showed that the failure occurred in an area of an intense clustering of small pre-earthquake landslides. The sturzstrom's debris crossed the valley, was ~130 m-thick and dammed two streams, producing extensive lakes. As of December 19, 2005, the lake in the Karli drainage was 800 m long and 20 m deep, and the lake in the Tang drainage was as 400 m long and 10 m deep (Harp and Crone, 2006). By 2008, both lakes have increased in size and depths, and the Pakistani government is draining the lakes to decrease the hazard of a lake outburst flood. Trommler et al. (2008) modeled the clear-water peak discharge of such a flood to be 8000 m^3/s causing a 12-m high flood wave immediately below the dam and 9-m high wave at the confluence of the Karli and Jhelum rivers near the village of Hattian.

Earthquake-triggered landslide and sturzstrom events that have dammed drainages have also been reported for other mountainous regions. Impressive examples include: Early Holocene sturzstroms in the Rhine Valley, Alps, impounded several lakes (Schneider et al., 2004; Pollet et al., 2005); in 1786, a $M=7.75$ earthquake occurred in Sichuan, southwestern China, resulting in a large landslide damming the Dadu River for ten days and a breakout flood that killed over 100,000 people (Dai et al., 2005); and the 1973 earthquake-triggered sturzstrom in Huascarán Norte, Peruvian Andes, resulted in ~23,000 deaths (Browning, 1973; Plafker and Ericksen, 1978). The most comprehensive inventory and bibliography of 463 landslide dams throughout the world was presented by Costa and Schuster (1991).

Owen et al. (2008) noted that many of the slopes throughout the region show little/no evidence of any landsliding or fissuring. They showed that these relatively stable slopes occurred: (i) mainly in the footwall rocks of the MBT; (ii) on mid slopes where the gradients are generally <20°, on both forested and deforested slopes; and (iii) on the steep and high, glaciated peaks between the Neelem and Kaghan rivers. Owen et al. (2008) concluded that, although earthquake-triggered landslides are abundant throughout an extensive area from the epicenter, they are concentrated in specific zones associated with the bedrock geology, geomorphology, topography and human factors. Furthermore, earlier studies in the Himalaya and other mountainous regions have also shown that earthquake-triggered landslides tend to concentrated in specific zones associated with the bedrock geology, geomorphology, topography, and human factors (Keefer, 1984, 1994, 1998; Owen et al., 1995, 1996; Rodriguez et al., 1999; Barnard et al. 2001; Jibson et al., 2004a, b). Landslides in the Himalaya can also be triggered non-earthquake mechanisms, including glacial debuttressing, fluvial undercutting, increased pore pressure during monsoon seasons, and human excavations (Barnard et al., 2001, 2004, 2006; Bookhagen et al., 2005; Dunning et al., 2007; Hewitt, 1998; Mitchell et al., 2007). For the Italian Apennine, Floris and Bozzano (2008) calculated annual rainfall-induced reactivation probabilities of ~0.1. Care must be taken, therefore, not to confuse earthquake-triggered landslides with other causes.

4. Event-controlling parameters

The occurrence of landslides in an earthquake area is a function of direct and indirect natural and human factors. These include, for example, lithology, structure, tectonics, geomorphology, topography, precipitation, temperature, infiltration, runoff, land cover, and road construction. These are commonly referred to as event-controlling parameters. The accuracy of geographical information system (GIS)-based susceptibility mapping is believed to increase with the availability of data about such event-controlling parameters (Ayalew et al., 2004). Unfortunately, for many susceptibility studies only limited data are available, and therefore, resulting susceptibility maps must be regarded with caution. Presently, however, susceptibility maps represent an accepted source for information on potential risks from natural hazards in a human environment.

Our examination of ASTER imagery that was taken on October 27, 2005 (Scene ID: SC:AST_L1A.003:2031456352) showed 2252 landslides covering a total of 61 km^2 within the study area. These landslides included pre- and post-earthquake events. Study and analysis of this image provide a general view of the relation between event-controlling parameters and landslide activity within the study area. However, it does not allow us to determine the number of landslides that occurred during and after the earthquake. In the following section, we describe the event-controlling parameters included in our study.

4.1. Lithology and faults

The 2005 earthquake's epicenter was located within the Indus–Kohistan seismic zone on the northwestern side of the Hazara–Kashmir Syntaxis along the NW-SE trending Kashmir Boundary Thrust (KBT), which was reactivated during the earthquake (Baig, 2006; Avouac et al., 2006; Yeats et al., 2006; Jayangondaperumal and Thakur, 2008) (Fig. 2). The earthquake's focal mechanism had slip/strike components consistent with the thrust faulting associated with the Hazara–Kashmir Syntaxis (Pararas, 2007). The mean slip is 5.1 m with a maximum slip of 9 m at depth of 4–8 km beneath Muzaffarabad (Bendick et al., 2007; Wang et al.; 2007); the rupture plane strikes NW-SE and dips NE 30° (Pathier et al., 2006). Synthetic Aperture Radar (SAR) data showed a 90 km-long belt of deformation along the KBT with a general vertical displacement of >1 m, with a maximum vertical displacement of 6 m north of Muzaffarabad (Fujiwara et al., 2006). Applying sub-pixel correlation of multi-temporal ASTER images, Avouac et al. (2006) concluded that the updip propagation of the rupture together with its steep dip angle and shallow distribution of slip must have contributed to the heavy damages in the near field. A ~300 m-wide zone of uplift and landslides across the KBT has been reported by the Geological Survey of Pakistan (Ahmed Hussain, pers. com. 2007).

The Geological Survey of Pakistan map (1:125,000; 1:50,000) includes eleven formations within the study area (Hussain and Khan, 1996; Hussain et al., 2004; Fig. 2, Table 1). The three major formations include the Murree, Hazara, and Salkhala Formations. The Murree Formation is the most extensive in the study area (>50%) and comprises Tertiary sedimentary rocks that vary from undeformed competent to tightly folded and highly cleaved and fractured beds, which at some locations include pencil cleavages. The Hazara Formation comprises highly fractured and cleaved slate, phyllite, shale and limestone and is located in the southwestern part of the study area. At many locations, the cleavage is tightly folded and pencil

Table 1
Landslides (LS) and geological formations within the study area of the 2005 Kashmir earthquake

Formation	Lithology	Area (km^2)	Area (%)	LS (number)	LS (%)	LS area (km^2)	Mean LS size (thousand m^2)	LS area in formation area (%)	LS per km^2
Alluvium	Alluvium	50	2.0	7	0.3	0.1	14.7	0.2	0.0
Hazara	Slate, shale, siltstone, limestone	284	11.3	123	5.9	2.0	16.3	0.7	0.4
Kamlial	Sandstone, shale, conglomerates	206	8.2	75	3.6	1.4	18.8	0.7	0.4
Kawagarh	Limestone	4	0.2	0	0.0	0.0	–	0.0	0.0
Mansehra	Intrusive rock, granite	145	5.8	66	3.2	0.7	11.0	0.5	0.5
Murree	Mudstone, siltstone, sandstone	1314	523	1327	63.4	30.6	23.1	2.3	1.0
Muzaffarabad	Dolomite, limestone, clastics	74	3.0	88	4.2	3.2	35.9	4.3	1.2
Panjal	Volcanics, metasediments	79	3.1	86	4.1	2.5	28.5	3.1	1.1
Salkhala	Limestone, marble	348	13.9	308	14.7	6.9	22.5	2.0	0.9
Samana Suk	Limestone	8	0.3	0	0.0	0.0	–	0.0	0.0
Tanawal	Quartzose schist, quartzite	4	0.2	13	0.3	0.1	6.1	2.0	3.3
All		(2517)	100	(2093)	100	(47.5)	22.7	(1.9)	(0.8)

The number of landslides here is only 2093 instead of 2252, since 159 landslides are part of more than one geologic formation and were excluded. Thus, some of the summarizing values are too low and these are shown in parentheses. In grey the most important number of each column.

cleavages are often developed. The Salkhala Formation comprises Precambrian metamorphic rocks and is present in the northeastern part of the study area. The remaining eight formations comprise a wide variety of rocks including granite, sandstone, siltstone, mudstone, conglomerate, schist, limestone and dolomite. The Muzaffarabad Formation is of particular note, comprising highly fractured dolomite and limestone in the lower portion of the hanging wall above the KBT around Muzaffarabad. Dissected and cannibalized Quaternary alluvial fans are very common throughout the region and reach up to several hundred meters thick radiating from the tributary valleys into the main trunk valley. These are particularly well developed and preserved around Muzaffarabad and to the north and east of the city.

Most (63%) of the landsliding in the study area occurred in the Murree Formation (Table 1). Large numbers (15%) of landslides also occurred in the Salkhala Formation, whereas, considerably fewer landslides occurred within the Hazara, Panjal, Kamlial, Mansehra, and Muzaffarabad Formations, and only a very few landslides occurred in the Tanawal and Samana Suk Formations and in the recent alluvium. The percentage of landslide-covered area within a geologic unit is highest (4.3%) in the Muzaffarabad Formation, which also has the largest (~36,000 m^2) mean landslide size. The Tanawal Formation has the highest density of landslides (>3/km^2).

In the GIS analysis buffer zones for fault lines (vector layer) were set to 100, 200, and 300 m. In the study area, a sample of 254 landslides, covering an area of 14 km^2 total showed that the number of landslides increases with increasing distance to the fault lines (6% within the 100 m zone; 9% within the 200 m zone; 11% within the 300 m zone). In the latter zone the average size of each landslide was 0.06 km^2. These results show that landsliding is more prevalent some distances (more than several hundred meters) away from the active fault traces.

4.2. Topography

A digital elevation model (DEM) with 15 m horizontal resolution was generated from the ASTER imagery using SILCAST 1.07 software. ESRI ArcGIS 9.2 software enabled the analysis of raster layers of primary topographic attributes from the DEM. These first and second derivates of elevation data include parameters such as slope, aspect, profile and plan curvatures (Moore et al., 1991). Elevation in the study area ranges from a minimum of ~450 m asl in some river beds and surrounding flood plains to a maximum of ~4450 m asl in the north-central part of the study area. A contour map with 500 m elevation intervals was generated and analyzed. More than half of the study area is at elevations of between 1000 and 2000 m asl; but only a few parts are lower than 1000 m asl (~12%) or higher than 3000 m asl (~6%) (Table 2).

Nearly 90% of all landsliding occurred at elevations below 2000 m asl, with nearly half of all landsliding being at elevations from 1000–1500 m asl. Only 10% of the landsliding occurred at elevations between 2000 and 3000 m asl, although ~30% of the study area is at these elevations. Furthermore, landsliding was scarce at high elevations above 3500 m asl.

Slope gradient is one of the most important factors in mass wasting: movement is extremely common when slopes are steeper than the natural angle of repose of the substrate and when there is no enough cohesion to inhibit slope failure. The angle of repose is typically 25–40° for unconsolidated materials. The occurrence of slope classes in the study area and the occurrence of landslides within each class are described in Table 3. The GIS work shows that most of the landsliding occurred on slopes of 25–35°. Landsliding is less on gentler (15–25°) and steeper (35–45°) slopes, with least occurring on very gentle (0–15°) and very steep (>45°) slopes.

Table 2
The relationship of landslides (LS) to elevation within the study area of the 2005 Kashmir earthquake

Elevation (m asl)	Area (km^2)	Area (%)	LS area (km^2)	LS area (%)	LS area in elevation (%)
0–500	0.2	>0.0	>0.0	0	5.7
500–1000	311	12.2	11.5	19	3.7
1000–1500	710	27.9	29.3	48	4.1
1500–2000	667	26.2	13.0	21	1.9
2000–2500	443	17.4	3.6	6	0.8
2500–3000	263	10.3	2.4	4	0.9
3000–3500	106	4.2	1.3	2	1.2
3500–4000	35	1.4	>0.0	0	>0.0
4000–4446	14	0.5	>0.0	0	>0.0
All	2549	100	61.1	100	2.4

In grey the most important number of each column.

Table 3
The relationship of landslides (LS) to slope gradient within the study area of the 2005 Kashmir earthquake

Slope (degrees)	Area (km^2)	Area (%)	LS area (km^2)	LS area (%)	LS area in slope (%)
0–15	566	22.2	4.3	7.1	0.8
15–25	637	25.0	18.1	29.7	2.8
25–35	795	31.2	25.1	41.0	3.2
35–45	455	17.8	12.7	20.7	2.8
45–90	96	3.8	0.9	1.5	0.9
All	2549	100	61.1	100	2.4

In grey the most important number of each column.

Table 4
The relationship of landslides (LS) to slope aspect within the study area of the 2005 Kashmir earthquake

Aspect	Area (km^2)	Area (%)	LS area (km^2)	LS area (%)	LS area in aspect (%)
North	307	12.0	0.2	0.3	0.1
Northeast	327	12.8	2.7	4.4	0.8
East	323	12.7	8.2	13.5	2.5
Southeast	325	12.7	13.1	21.5	4.0
South	326	12.8	12.3	20.1	3.8
Southwest	328	12.9	18.1	29.7	5.5
West	299	11.7	4.7	7.7	1.6
Northwest	314	12.3	1.8	2.9	0.6
All	2549	100	61.1	100	2.4

In grey the most important number of each column.

Slope aspect has an effect on landsliding because it is related to such factors as insolation (weathering), weather conditions (precipitation, snow meltwater), land cover (forest, grassland, brush land, agricultural land), and soil conditions (infiltration capacity). The satellite image and DEM analyses for the study area revealed that there are more southwestern and western facing slopes than other directions. Furthermore, most of the landsliding (>70%) occurred on slopes facing southerly directions (southeast, south, southwest; Table 4). Precipitation might be higher on southern slopes due to the higher monsoon rainfall and on western slopes as a result of the westerlies, which enhances slope instability.

4.3. Land cover

The October 2005 ASTER imagery was used to develop a supervised land cover classification (raster layer), i.e., identified classes in the satellite analysis were compared with field observations for selected detailed study sites. Ground truth data were collected in the field in November 2005 by driving and hiking through the region. This was supplemented by surveys during a helicopter flight over the remote parts of the study area. These surveys included the development of a landslide inventory, and photographs and GPS measurements of the landslide locations.

The software used for our analyses, IDRISI Andes, includes several land cover classification techniques. Three of them (Maxlike, Fisher, Multi-Layer Perception) were compared to assess accuracy. Multi-Layer Perception (MLP), a neural network method, produced the best overall results (72% accuracy) and was used for our land cover classification of the study area. Seven final land cover classes were identified, including water; urban areas; snow/ice; forest; shrub land/grassland; agriculture; and unclassified.

The landscape is dominated by forest and shrub land/grassland (Table 5). Agricultural land is restricted to river terraces and alluvial fans along the valleys floors, and terraced steeper slopes. The urban areas mainly occur along the rivers, and include three larger urban centers (Muzaffarabad, Balakot, and Hattian). Snow/ice is only present on some of the higher ridges to the north. The results of our land cover classification are very similar to those of the AJK Forest Department (2001), which defined 42% forest, 42% uncultivable land mainly for grazing, 13% cultivated land and 3% urbanized area. In our analysis, 2.4% of the entire study area is covered by landslides. The majority of landsliding occurred in shrub land/grassland (<70%) and on agricultural land (20%). However, few (2%) landsliding occurred in forested areas.

4.4. Rivers and roads

A GIS dataset for rivers and roads was obtained from the United Nations Joint Logistic Center (UNJLC) in Islamabad. This dataset, however, was incomplete and proved inaccurate when examined at scales of 1:100,000 or greater. The datasets (vector layers), therefore, had to be manually corrected and completed for all main and tributary valleys using the ASTER imagery. The road dataset remained incomplete for small areas located to the west of the Jhelum and Kunhar rivers due to problems of identifying smaller roads in the ASTER imagery. Thus, for the road network in those parts of the study area the final susceptibility map has to be considered with care.

Van Westin et al. (2003) suggested that buffer zones for line features, such as, rivers and roads should be set to 50 m (on each side of the line feature). Many of the roads in the steep study area, however, are actually built close to rivers, within a buffer zone of 50 m, and include failures related to either rivers or roads. In our study, therefore, the buffer zones were set to 25 m and 50 m.

The GIS work showed that much of the landsliding occurred within the buffer zones along rivers or roads within our study area (Fig. 3): ~30% of all landsliding happened in the 25-m buffer zone along rivers compared to ~20% along roads (both numbers increase by 6% for the 50-m buffer zone). These results highlight the human impact and effect on slope failures and support the views of Owen et al. (2008) and Sudmeier-Rieux et al. (2007a) who argued that human factors contributed to a large percentage of slope failures. Owen et al. (2008) showed that >50% of the landslides they examined were related to human terracing and excavations for building and road constructions. Similarly, Sudmeier-Rieux et al. (2007a) concluded that 56% of landslides in the lower Neelum Valley were caused by human-induced factors, especially deforestation, poor terracing and habitations located on exposed slopes, and road construction. The negative impact of road construction on slope stability resulting in landsliding has also been described for other mountainous regions (Swanson and Dyrness, 1975; Ives and Messerli, 1989; Jones et al., 2000; Barnard et al., 2001; Borga et al., 2005; Lozano et al., 2005; Moreiras, 2006).

5. Multi-Criteria Evaluation (MCE)

Multi-Criteria Evaluation (MCE) is a decision support tool used within the realm of GIS. The decision is a choice between alternatives or identifying priorities (landslide susceptibility). For the latter a set of factors or attributes (event-controlling parameters such as slope and land cover) are evaluated and weighted to generate criterions. MCE merely combines these criteria to construct a single composite that can be used for decision making for a specific objective (Malczewski, 1999). The objective for this MCE is to assess the designated study area to determine landslide susceptibility.

MCE employs a number of different qualitative or statistical methods, such as, Analytical Hierarchy Process (AHP; Saaty, 1990; Yagi, 2003), Likelihood Frequency Ratio (LRM; Akgün et al., in press), Logistic Regression (LR; Akgün and Bulut, 2007), Multivariate Statistical Approach (MSA; Ayalew and Yamagishi, 2004; Carrara et al., 2008), and Weighted Linear Combination (WLC; Jiang and Eastman, 2000; Ayalew et al., 2004; Akgün et al., in press). This study

Table 5
The relationship of landslides (LS) to land cover within the study area of the 2005 Kashmir earthquake

Land cover	Area (km^2)	Area (%)	LS area (km^2)	LS area (%)	LS area in land cover (%)
Water	35	1.4	0.0	0.0	0.0
Urban	14	0.5	0.0	0.0	0.0
Snow/ice	27	1.1	0.2	0.3	0.8
Forest	1148	45.0	1.4	2.3	0.1
Shrubs/grassland	1068	41.9	41.1	67.3	3.8
Agriculture	164	6.4	12.0	19.7	7.3
Unclassified	94	3.6	6.3	10.4	-
All	2549	100	61.1	100	2.4

In grey the most important number of each column.

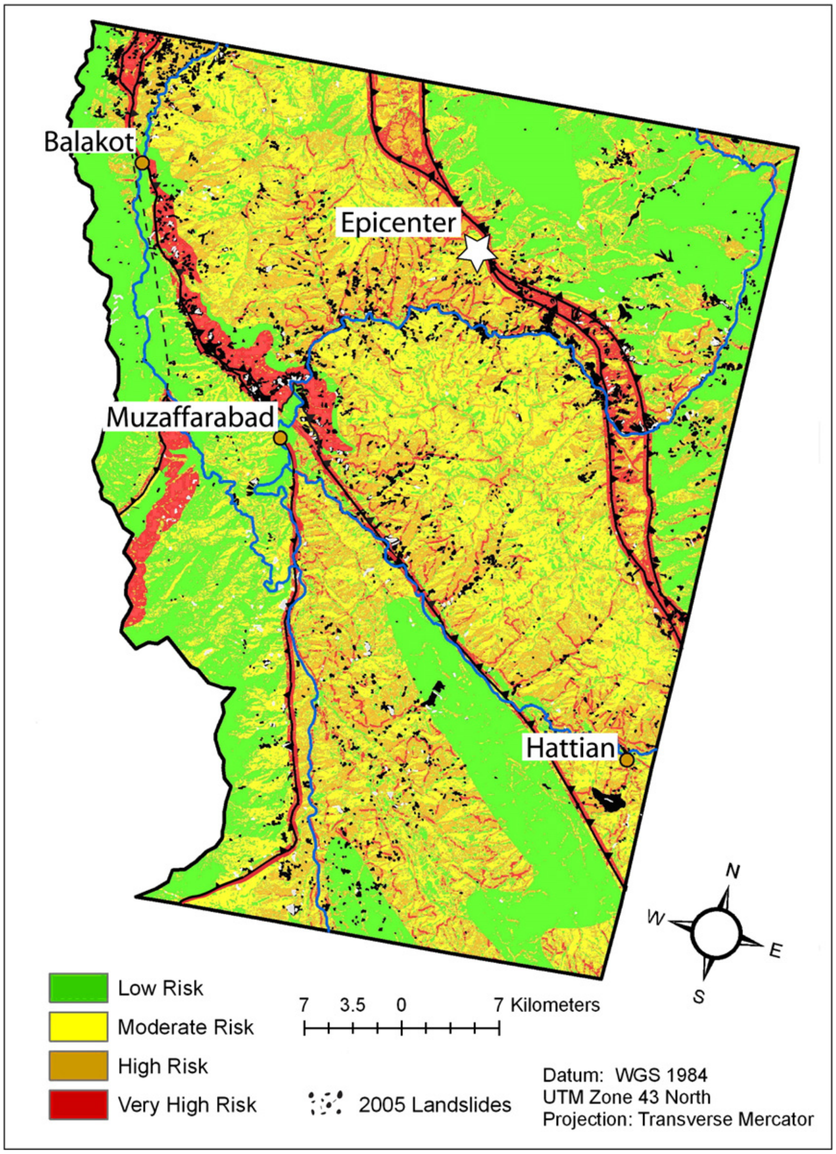

Fig. 3. Landslide susceptibility map of our 2005 Kashmir earthquake study area. Two-thirds of the study area has a low or moderate susceptibility to future landsliding, while the other third has a high or very high susceptibility to future slope failures. The highest susceptibility to future failures occurs in regions that are underlain by the Muzaffarabad Formation, followed by the Murree and Panjal Formations (see Fig. 2). Future landsliding is predicted for all areas that are in some proximity to faults, rivers or roads. (The color version of this figure is available in the web version of this article.)

will make use of the AHP method because of its precision, ease of use, and because of its ready availability as a built-in tool within IDRISI Andes software. AHP considers only a one-level weighting system developed by collecting expert opinions, in this case our experience obtained during the field work in November 2005. Thus, here the applied method contains some elements of subjectivity, which is also true for many other susceptibility mapping approaches (e.g., Rock Engineering System (RES) method after Hudson, 1992; modified in Budetta et al., 2008).

Factor weights for each criterion are determined by a pair-wise comparison matrix as described by Saaty (1990, 1994) and Saaty and Vargas (2001). The method employs an underlying 9-point recording scale to rate the relative preference on a one-to-one basis of each criteria (Malczewski, 1999). For better map presentation purposes the scale assigns a linguistic expression to each corresponding numerical value (Table 6). When using this approach, it is commonly accepted that taking numerical values and assigning them such linguistic expressions that translate into an imprecise terminology creates a vast area of ambiguity about the results. In most susceptibility assessments, however, the state of knowledge about all event-controlling parameters is simply imperfect anyway. The numerical values are quantified translations useful for calculating factor weights and the validity of the numerical values may best be judged by the factor weights and the consistency of the calculation process (Ayalew et al., 2004). Pair-wise comparison, however, is subjective and the quality of the results is highly dependant on the expert's judgment.

Table 6
Pair-wise comparison 9-point rating scale

Importance	Definition	Explanation
1	Equal importance	Contribution to objective is equal
3	Moderate importance	Attribute is slightly favored over another
5	Strong importance	Attribute is strongly favored over another
7	Very strong importance	Attribute is very strongly favored over another
9	Extreme importance	Evidence favoring one attribute is of the highest possible order of affirmation
2, 4, 6, 8	Intermediate values	When compromise is needed

Table 7
Pair-wise comparison matrix for calculating factor weights

Attribute	Aspect	Elevation	Faults	Lithology	Land cover	Rivers	Roads	Slope	Tributaries	Factor weights
Aspect	1									0.0267
Elevation	2	1								0.0358
Faults	6	5	1							0.1607
Lithology	7	6	3	1						0.2840
Land cover	4	4	1/3	1/5	1					0.0790
Rivers	4	4	1/3	1/5	1	1				0.0790
Roads	4	4	1/3	1/5	1	1	1			0.0790
Slope	7	5	2	1	4	4	4	1		0.2389
Tributaries	1/3	1/4	1/7	1/8	1/6	1/6	1/6	1/8	1	0.0169

The consistency ratio (CR) for this study is 0.05.

The results of the pair-wise comparison matrix and the factor weights are shown in Table 7. The quality of the comparison is described by the consistency ratio (CR), which is a ratio between the matrix's consistency index and random index. This ranges from 0 to 1. A CR close to 0 indicates the probability that the matrix's rating was randomly generated. Saaty (1990) recommended the CR to be <0.1 to be valid. The CR in our study is 0.05. Lithology is the most heavily weighted factor followed by slope and faults. Aspect and elevation are the least contributing event-controlling parameters, while land cover, rivers, and roads have a moderate influence. These results support the view that lithology and tectonics are the most influential event-controlling parameters for landsliding in tectonic active regions (e.g., Brabb, 1984).

6. The landslide susceptibility map

The final susceptibility map was created in IDRISI Andes and exported into ESRI ArcMap 9.2 (Fig. 3). For quality assessment, the landslide susceptibility map was compared with the occurrence of landslides determined from the satellite analysis. The result is the susceptibility success rate that illustrates the success of the map in predicting landsliding throughout the study area (Chung and Fabbri, 1999; Lee, 2004; Zêzere et al., 2004; Saha et al. 2005; Conoscenti et al., 2008; Fig. 4). The higher the percentage of the area below the curve, i.e. the steeper the curve's slope, the better is the prediction. The accuracy of our landslide susceptibility map is 67%, which is acceptable for the prediction.

The landslide susceptibility success rate was also used to define the four relative susceptibility classes. These were described by verbal susceptibility expressions and colors: low (green), moderate (yellow), high (orange), and very high (red). Table 8 describes how much of the study area is in each of the four susceptibility classes. Two-thirds of the study area has a low or moderate susceptibility to future landsliding, while the other third has a high or very high susceptibility to future slope failures. The highest susceptibility to future failures occurs in regions that are underlain by the Muzaffarabad Formation, followed by the Murree and Panjal Formations. Sudmeier-Rieux et al. (2007a) note that the Murree Formation is characterized by impermeability and is susceptible to landslides due to rainfall. According to our map, future landsliding is also predicted for all areas that are in some proximity to faults. The strip between Muzaffarabad and Balakot (including the two cities themselves) is extremely unsafe because it comprises the Muzaffarabad Formation and runs along the KTB. In general, safer areas are to be found west of the Jhelum and Kunhar rivers and in the northeast of the study area. The triangle that is enclosed by the Jhelum River has safer areas within the Kamlial Formation. In general, an increased threat also exists in close proximity to rivers and roads (Fig. 5).

Most of the destruction within Muzaffarabad City was a direct result of the earthquake itself and of earthquake-triggered landsliding (although landslides destroyed buildings and roads in the outskirts). Therefore, the alluvium that makes up most of the city area has a low susceptibility to future landsliding (Fig. 6). The area towards the west of Muzaffarabad comprises the Hazara Formation and has a low to

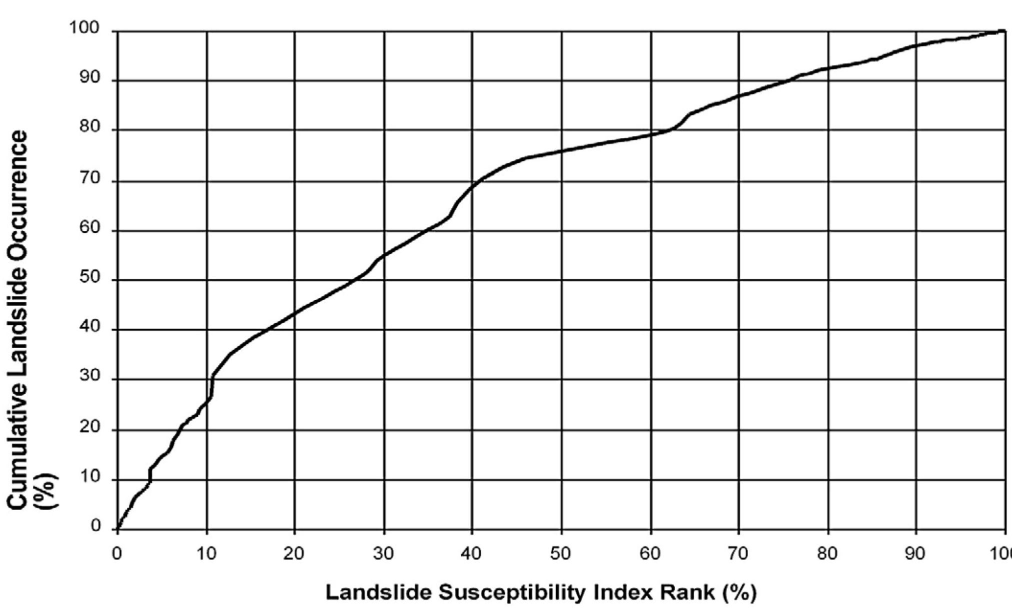

Fig. 4. Success rate for the landslide susceptibility mapping in our study area in the 2005 Kashmir earthquake region. The accuracy of our landslide susceptibility map is 67%, which is acceptable for the prediction.

Table 8
Susceptibility to landsliding for the study area of the 2005 Kashmir earthquake

CLO (%)	Susceptibility class	Area (km^2)	Area (%)
0–20	Low	969	38.0
20–40	Moderate	737	28.9
40–70	High	577	22.7
70–100	Very high	266	10.4

CLO = Cumulative Landslide Occurrence.

moderate landslide susceptibility. Towards the east of the city, areas comprising the Murree Formation have a moderate to high landslide susceptibility. Very high landslide susceptibility is identified for areas comprising the Muzaffarabad Formation towards the north and northwest of the city and along the fault lines. In the surrounding of Muzaffarabad City, high to very high landslide susceptibility is predicted for most areas in close proximity to rivers and roads.

7. Conclusion

During an earthquake slopes are subject to failure and can constitute a landsliding hazard. Hence it is important to assess these slopes for future potential failure. Our study of the region effected by the October 8, 2005 Kashmir earthquake showed that the bedrock lithology is the most influential and important landsliding-controlling parameter. Most of the landslides occurred in highly fractured shale, slate, clastic sediments, and limestone and dolomite, mainly of the Murree and Salkhala Formations. Slope gradient had the second highest influence as an event-controlling parameter, and most of the landslides occurred on slopes from 25–35°. Landsliding increased towards the active faults, although only one out of ten failures occurred within a 300-m buffer zone. Aspect and elevation were the least influential parameters affecting landsliding; but most of the failures occurred at moderate elevations of 1000–1500 m asl on southern slopes facing the summer monsoon precipitation. Shrub land, grassland, and also agricultural land were highly susceptible to

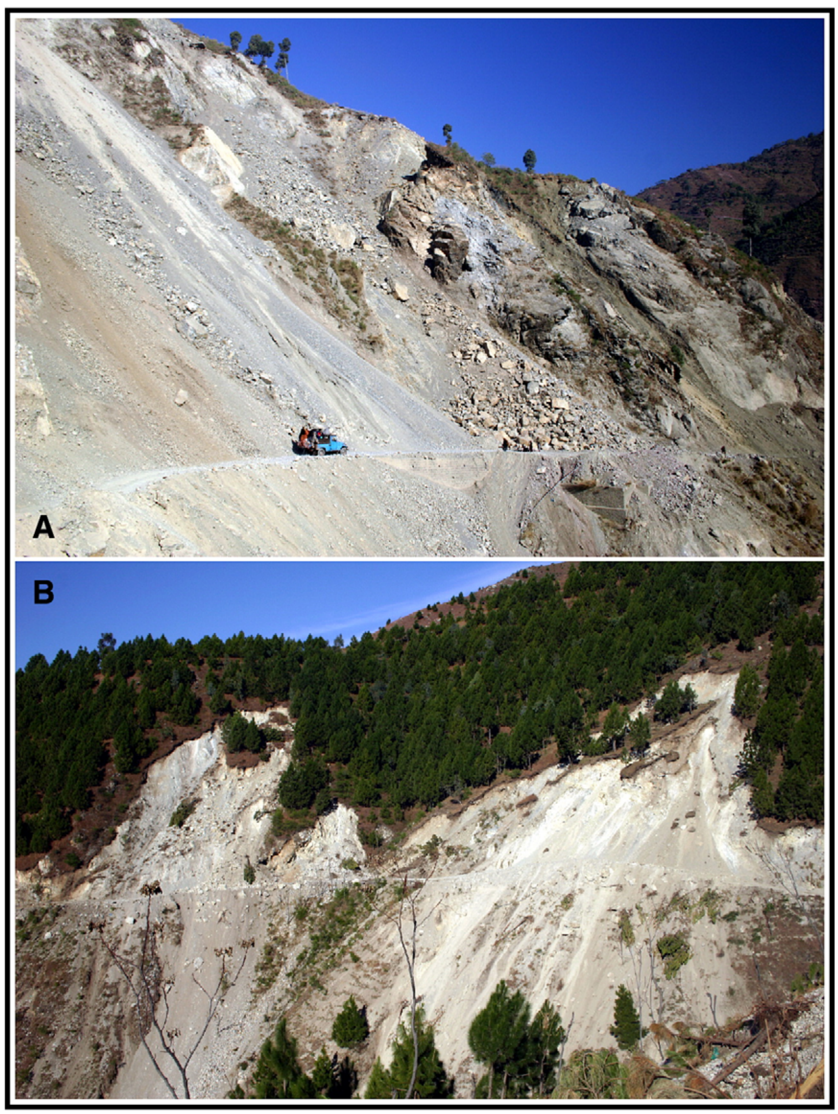

Fig. 5. Landsliding and landslide susceptibility in the study area of the 2005 Kashmir earthquake (for locations of A and B see Fig. 6). (A) Very high landslide susceptibility in a reactivated landslide area in the Neelum Valley north of Muzaffarabad. The road is the main line of transportation in the Neelum Valley and was affected by landsliding in numerous locations; mainly rock fall deposits blocked the road repeatedly for several days. (B) Very high landslide susceptibility along a road east of Muzzafarabad. In both examples A and B, very high susceptibility to ongoing landsliding is predicted due to the proximity to the Kashmir Boundary Thrust (<2 km), the Muzaffarabad Formation (dolomite, limestone, clastics), the steepness of the terrain, and the road itself. In example A, the Neelum River (fluvial lateral erosion) contributes to the negative evaluation. In example B, the landsliding happened on a slope covered with forest, although few (2%) landslides occurred in forested areas. (The color version of this figure is available in the web version of this article.)

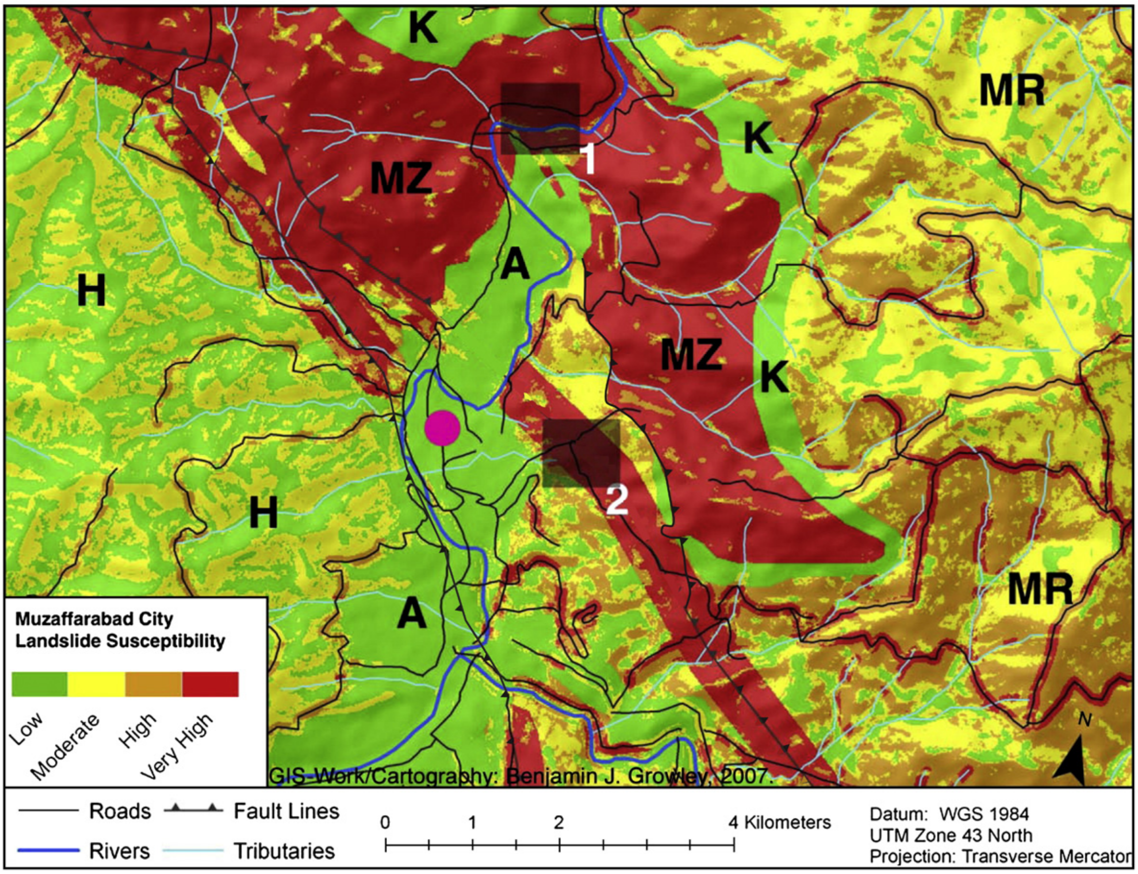

Fig. 6. Landslide susceptibility around Muzaffarabad, the district capital of the state of Azad Jammu and Kashmir in northern Pakistan (pink spot: center of Muzaffarabad; box 1: see Fig. 5A; box 2: see Fig. 5B). The epicenter lies ~10 km northeast of the city. The alluvium ("A") that makes up most of the city area has a low susceptibility to future landsliding. Low landslide susceptibility is also predicted for areas comprising the Kamlial Formation ("K"). The area towards the west of Muzaffarabad comprises the Hazara Formation ("H") and has a low to moderate landslide susceptibility. The area towards the east comprises the Murree Formation ("MR") and is characterized by a moderate to high landslide susceptibility. Very high landslide susceptibility is identified for areas comprising the Muzaffarabad Formation ("MZ") and along the fault lines. High to very high landslide susceptibility is predicted for most areas in close proximity to rivers and roads. (For interpretation of the references to color in this figure legend, the reader is referred to the web version of this article.)

failures, while forest cover seemed to effectively protect from landsliding. Many of the failures occurred along rivers (every third failure) and roads (every fifth failure) cut into the slopes. Thus, in this region of the Himalaya, deforestation and road construction seemed to have a strong negative impact on landscape stability during the earthquake. This is an important point since protective measures against the hazard of earthquake-triggered landslides should focus on deforested regions and along highways. Sudmeier-Rieux et al. (2007a) made similar conclusions: in their susceptibility map for the lower Neelum Valley the main contributors to landsliding were slopes, proximity to fault lines, and roads/trails. The study also revealed that area covered by forests suffered much fewer landslides than deforested areas.

Although the majority of the study area is only low or moderately susceptible to future landsliding, one-third is indeed high or even highly susceptible. Unsafe areas are related to regions underlain by the Kingrali, Murree, and Panjal Formations, and to active faults. The cities Muzaffarabad and Balakot and the strip between them are unsafe and it is likely that future landsliding will continue in this region. These unsafe areas require immediate mitigation action. Reactivation of existing landslide sites and new landsliding, particularly along fissures, occurs following monsoon rains and snowmelt. In 2006, Bulmer et al. (2007) detected downslope and across-slope movement of landslide study sites over a timescale of a few days, a period during which heavy monsoon rainfalls began. Bulmer et al. (2007) stated that a number of deep-seated landslides will continue to pose severe threat to roads and adjacent villages. Unusually heavy rains in March 2007 triggered a number of slides on slopes with active landslides and fissures (Sudmeier-Rieux et al., 2007b).

Our susceptibility map can provide a cheap and comprehensive assessment of the likelihood of future failures, which can be useful to planners for the rebuilding process and future zoning issues. Individual landslide areas can be remediated by employing engineering techniques, such as, the use of retaining wall, but these are expensive and need continuous monitoring. Data for future waterworks, building construction, and electrical lines, however, can be incorporated into our landslide susceptibility GIS securing the best possible location concerning precautionary landslide safety. Furthermore, we hope that our study will provide a model for predicting earthquake-triggered and other landslides in adjacent regions of the Himalaya and other high mountain regions.

Acknowledgements

We thank the National Science Foundation (EAR-0602675) and The University of Montana for financial support, Mrs. Aisha Khan (Mountain and Glacier Protection Agency, Islamabad), Major General Nadeem Ahmed and the Pakistan Army for field support. Thanks to the United Nations Joint Logistic Centre (UNJLC) in Islamabad for some GIS data and to Jeffrey Olsenholler (University of Nebraska-Omaha) for ASTER DEM generation. Thanks to Anna Klene and Rebecca Bendick, The University of Montana, for suggestions for data analyses and interpretations. Thanks to two anonymous reviewers and Richard Marston for helpful comments.

References

Abbott, P.L., 2007. Natural disasters. McGraw Hill, San Diego. 510 pp.

AJK Forest Department, 2001. Forestry Statistics of Azad Kashmir.

Akgün, A., Bulut, F., 2007. GIS-based landslide susceptibility for Arsin-Yomra (Trabzon, North Turkey) region. Environmental Geology 51, 1377–1387.

Akgün, A., Dag, S., Bulut, F., in press. Landslide susceptibility mapping for a landslide-prone area (Findikli, NE of Turkey) by likelihood-frequency ratio and weighted linear combination models. Environmental Geology. doi:10.1007/s00254-007-0882-8.

Alexander, D.E., 2005. Vulnerability to landslides. In: Glade, T., Anderson, M., Crozier, M.J. (Eds.), Landslide Hazard and Risk. Wiley, Chichester, UK, pp. 175–198.

Alexander, D.E., 2008. A brief survey of GIS in mass-movement studies, with reflections on theory and methods. Geomorphology 94, 261–267.

Anbalagan, R., 1992. Landslide hazard evaluation and zonation mapping in mountainous terrain. Engineering Geology 32, 269–277.

Avouac, J.-P., Ayoub, F., Leprince, S., Konca, O., Helmberger, D.V., 2006. The 2005, M_w 7.6 Kashmir earthquake: sub-pixel correlation of ASTER images and seismic waveforms analysis. Earth and Planetary Science Letters 249, 514–528.

Ayalew, L., Yamagishi, H., 2004. The application of GIS-based logistic regression for landslide susceptibility mapping in the Kakuda–Yahiko Mountains, Central Japan. Geomorphology 65, 15–31.

Ayalew, L., Yamagishi, H., Ugawa, N., 2004. Landslide susceptibility mapping using GIS-based weighted linear combination, the case in Tsugawa area of Agano River, Niigata Prefecture, Japan. Landslides 1, 73–81.

Baig, M.S., 2006. Active faulting and earthquake deformation in Hazara–Kashmir Syntaxis, Azad Kashmir, northwest Himalaya. In: Kausar, A.B., Karim, T., Khan, T. (Eds.), International Conference on 8 October 2005 Earthquake in Pakistan: Its Implications & Hazard Mitigation, January 18–19, 2006, Islamabad, Extended Abstracts, pp. 27–28.

Barnard, P.L., Owen, L.A., Sharma, M.C., Finkel, R.C., 2001. Natural and human-induced landsliding in the Garwhal Himalaya of northern India. Geomorphology 40, 21–35.

Barnard, P.L., Owen, L.A., Sharma, M.C., Finkel, R.C., 2004. Late Quaternary landscape evolution of a monsoon-influenced high Himalayan valley, Gori Ganga, Nanda Devi, NE Garhwal. Geomorphology 61, 91–110.

Barnard, P.L., Owen, L.A., Finkel, R.C., 2006. Quaternary fans and terraces in the Khumbu Himal south of Mount Everest: their characteristics, age and formation. Journal of Geological Society of London 163, 383–399.

Bendick, R., Bilham, R., Khan, M.A., Khan, S.F., 2007. Slip on an active wedge thrust from geodetic observations of the 8 October 2005 Kashmir earthquake. Geology 35, 267–270.

Bhatnagar, P.S., 1998. Landslide zonation mapping in parts of Chamba and Kangra districts, Himachal Pradesh; a refinement of existing methodology. Journal of Engineering Geology 26, 81–88.

Bookhagen, B., Thiede, R.C., Strecker, M.R., 2005. Late Quaternary intensified monsoon phases control landscape evolution in the northwest Himalaya. Geology 33, 149–152.

Borga, M., Tonelli, F., dalla Fontana, G., Cazorzi, F., 2005. Evaluating the influence of forest roads on shallow landsliding. Ecological Modelling 187, 85–98.

Brabb, E.E., 1984. Innovative approaches to landslide hazard mapping. Proceedings of 5th International Symposium on Landslides, Rotterdam, pp. 1059–1074.

Browning, J.M., 1973. Catastrophic rock slide, Mount Huascaran, Peru, May 31, 1970. American Association of Petroleum Geologists Bulletin 57, 1335–1341.

Budetta, P., Santo, A., Vivenzio, F., 2008. Landslide hazard mapping along the coastline of the Cilento region (Italy) by means of a GIS-based parameter rating approach. Geomorphology 94, 340–352.

Bulmer, M., Farquhar, T., Roshan, M., Akhtar, S.S., Wahla, S.K., 2007. Landslide hazards after the 2005 Kashmir earthquake. Eos Transactions 88, 53.

Calkins, A.J., Offield, W.T., Abdullah, S.K.M., Ali, S.T., 1975. Geology of the southern Himalaya in Hazara, Pakistan and adjacent areas. US Geological Survey Professional Paper 716-C, Denver, Colorado. 29 pp.

Carrara, A., Crosta, G., Frattini, P., 2008. Comparing models of debris-flow susceptibility in the alpine environment. Geomorphology 94, 353–378.

Chacon, J., Irigaray, C., Fernandez, T., El Hamdouni, R., 2006. Engineering geology maps: landslides and geographical information systems. Bulletin Engineering Geology and Environment 65, 341–411.

Chung, C.-J.F., Fabbri, A.G., 1999. Probabilistic prediction models for landslide hazard mapping. Photogrammetric Engineering and Remote Sensing 65, 1389–1400.

Conoscenti, C., Di Maggio, C., Rotiglinao, E., 2008. GIS analysis to assess landslide susceptibility in a fluvial basin of NW Sicily (Italy). Geomorphology 94, 325–339.

Costa, J.E., Schuster, R.L., 1991. Documented historical landslide dams from around the world. U.S. Geological Survey Open-File Report 91-239. 486 pp.

Dai, F.C., Lee, C.F., 2002. Landslide characteristics and slope instability modeling using GIS, Lantau Island, Hong Kong. Geomorphology 42, 213–238.

Dai, F.C., Lee, C.F., Deng, J.H., Tham, L.G., 2005. The 1786 earthquake-triggered landslide dam and subsequent dam-break flood on the Dadu River, southwestern China. Geomorphology 65, 205–221.

District Census Report, 1998. Population Census Organization. Islamabad, Pakistan.

Dunning, S.A., Mitchell, W.A., Rosser, N.J., Petley, D.N., 2007. The Hattian Bala rock avalanche and associated landslides triggered by the Kashmir earthquake of 8 October 2005. Engineering Geology 93, 130–144.

EERI (Earthquake Engineering Research Institute), 2005. First Report on the Kashmir Earthquake of October 8, 2005. http://www.eeri.org/lfe/clearinghouse/kashmir/reports/kashmir_eeri_1st_report.pdf accessed 15 February 2006.

Espizua, L.E., Bengochea, J.D., 2002. Landslide hazard and risk zonation mapping in the Río Grande Basin, Central Andes of Mendoza, Argentina. Mountain Research and Development 22, 177–185.

Floris, M., Bozzano, F., 2008. Evaluation of landslide reactivation: a modified rainfall threshold model based on historical records of rainfall and landslides. Geomorphology 94, 40–57.

Fujiwara, S., Tobita, M., Sato, H.P., Ozawa, S., Une, H., Koarai, M., Nakai, H., Fujiwara, M., Yarai, H., Nishimura, T., Hayashi, F., 2006. Satellite data gives snapshot of the 2005 Pakistan Earthquake. Eos Transactions 87, 73 and 77.

Harp, E.L., Crone, A.J., 2006. Landslides triggered by the October 8, 2005, Pakistan earthquake and associated landslide-dammed reservoirs. U.S. Geological Survey Open-File Report 2006-1052. 10 pp.

Hewitt, K., 1998. Catastrophic landslides and their effects on the Upper Indus streams, Karakoram Himalaya, northern Pakistan. Geomorphology 26, 47–80.

Hudson, J.A., 1992. Rock Engineering Systems: Theory & Practice. High Plains Press (JAH), Chichester, UK, p. 185.

Hussain, A., Khan, R.N., 1996. Geological map of Azad Jammu and Kashmir. Geological Map Series. Geological Survey of Pakistan, Islamabad.

Hussain, A., Mughal, N., Haq, I., Latif, A., 2004. Geological map of the Garhi Habibullah area, district Mansehra and parts of Muzaffarabad district, AJK. Geological Map Series. Geological Survey of Pakistan, Islamabad.

Ives, J., Messerli, B., 1989. The Himalayan Dilemma. Reconciling Development and Conservation. United Nations University Press, Tokyo. 324 pp.

Jayangondaperumal, R., Thakur, V.C., 2008. Co-seismic secondary surface fractures on southeastward extension of the rupture zone of the 2005 Kashmir earthquake. Tectonophysics 446, 61–76.

Jiang, H., Eastman, J.R., 2000. Application of fuzzy measures in multi-criteria evaluation in GIS. International Journal of Geographic Information Science 14, 173–184.

Jibson, R.W., Crone, A.J., Harp, E.L., Baum, R.L., Major, J.J., Pullinger, C.R., Escobar, C.D., Marinez, M., Smith, M.E., 2004a. Landslides triggered by the 13 January and 13 February 2001 earthquakes in El Salvador. In: Bommer, J.J., Rose, W.I., López, D.L., Carr, M.J., Major, J.J. (Eds.), Natural Hazards in El Salvador. Geological Society of America Special Paper 375, Boulder, Colorado, pp. 69–88.

Jibson, R.W., Harp, E.L., Schulz, W., Keefer, D.K., 2004b. Landslides triggered by the 2002 Denali Fault, Alaska, earthquake and the inferred nature of the strong shaking. Earthquake Spectra 20, 669–691.

Jones, J.A., Swanson, F.J., Wemple, B.C., Snyder, K.U., 2000. Effects of roads on hydrology, geomorphology, and disturbance patches in stream networks. Conservation Biology 14, 76–85.

Joshi, V., Murthy, T.V.R., Arya, A.S., Narayana, A., Naithani, A.K., Garg, J.K., 2003. Landslide hazard zonation of Dharasu–Tehri–Ghansali area of Garhwal Himalaya, India using remote sensing and GIS techniques. Journal of Nepal Geological Society 28, 85–94.

Kazmi, A.H., Jan, Q.M. (Eds.), 1997. Geology and tectonics of Pakistan. Graphic Publisher, Karachi, Pakistan. 554 pp.

Keefer, D.K., 1984. Landslides caused by earthquakes. Geological Society of America Bulletin 95, 406–421.

Keefer, D.K., 1994. The importance of earthquake-induced landslides to long-term slope erosion and slope-failure hazards in seismically active regions. Geomorphology 10, 265–284.

Keefer, D.K. (Ed.), 1998. The Loma Prieta, California, earthquake of October 17, 1989, Landslides. US Geological Survey Professional Paper 1551-C. U.S. Geological Survey, Denver, Colarodo. 185 pp.

Lee, S., 2004. Application of artificial neural network for landslide susceptibility mapping at Janghung, Korea. International Geological Congress, Abstracts 32, Part 1, pp. 76–77.

Lee, S., Min, K., 2001. Statistical analysis of landslide susceptibility at Yongin, Korea. Environmental Geology 40, 1095–1113.

Lozano, P., Bussmann, R.W., Küppers, M., 2005. Landslides as ecosystem disturbance — their implications and importance in South Ecuador. Lyonia 8, 67–72.

Malczewski, J., 1999. GIS and multicriteria decision analysis. John Wiley & Sons, New York. 408 pp.

Mitchell, W.A., McSaveney, M.J., Zondervan, A., Kim, K., Dunning, D.A., Taylor, P.J., 2007. The Keylong Seri rock avalanche, NW Indian Himalaya: geomorphology and palaeoseismic implications. Landslides 4, 245–254.

Moore, I.D., Grayson, R.B., Ladson, A.R., 1991. Digital terrain modeling: a review of hydrological, geomorphological and biological applications. Hydrological Processes 5, 3–30.

Moreiras, S.M., 2006. Frequency of debris flows and rockfall along the Mendoza river valley (Central Andes), Argentina: associated risk and future scenario. Quaternary International 158, 110–121.

Owen, L.A., Sharma, M.C., Bigwood, R., 1995. Mass movement hazard in the Garhwal Himalaya: the effects of the 20 October 1991 Garhwal earthquake and the July–August 1992 monsoon season. In: McGregor, D.F.M., Thompson, D.A. (Eds.), Geomorphology and Land Management in a Changing Environment. Wiley, Chichester, UK, pp. 69–88.

Owen, L.A., Sharma, M., Bigwood, R., 1996. Landscape modification and geomorphological consequences of the 20 October 1991 earthquake and the July–August 1992 monsoon in the Garhwal Himalaya. Zeitschrift für Geomorphologie 103, 359–372.

Owen, L.A., Kamp, U., Khattak, G.A., Harp, E.L., Keefer, D.K., Bauer, M.A., 2008. Landslides triggered by the October 8, 2005, Kashmir earthquake. Geomorphology 94, 1–9.

Pachauri, A.K., Gupta, P.V., Chander, R., 1998. Landslide zoning in a part of the Garhwal Himalayas. Environmental Geology 36, 325–334.

Pakistan Water Gateway, 2007. Jhelum River: Key Facts. http://waterinfo.net.pk/fsrj.htm accessed 11 November 2007.

Pararas, G., 2007. The earthquake of 8 October 2005 in Northern Pakistan. http://www.drgeorgepc.com/Earthquake2005Pakistan.html accessed 22 February 2007.

Pathier, E., Fielding, E.J., Wright, T.J., Walker, R., Parsons, B.E., Hensley, S., 2006. Displacement field and slip distribution of the 2005 Kashmir earthquake from SAR imagery. Geophysical Research Letters 33, L20310. doi:10.1029/2006GL027193.

Peiris, N., Rossetto, T., Burton, P., Mahmood, S., 2006. EEFIT Mission: October 8, 2005 Kashmir Earthquake. Published Report, The Institution of Structural Engineers, London, U.K. 31 pp.

Plafker Ericksen, 1978. Nevados Huascaran avalanches. In: Voight, B. (Ed.), Rockslides and Avalanches. Natural Phenomena, vol. 1. Elsevier, New York, pp. 277–314.

Pollet, N., Cojean, R., Couture, R., Schneider, J.-L., Strom, A.L., Voirin, C., Wassmer, P., 2005. A slab-on-slab model for the Flims rockslide (Swiss Alps). Canadian Geotechnical Journal 42, 587–600.

Remondo, J., Bonchea, J., Cendrero, A., 2008. Quantitative landslide risk assessment and mapping on the basis of recent occurrences. Geomorphology 94, 496–507.

Rodriguez, C.E., Bommer, J.J., Chandler, R.J., 1999. Earthquake induced landslides: 1980–1997. Soil Dynamics Earthquake Engineering 18, 325–346.

Saaty, T., 1990. The analytic hierarchy process: planning, priority setting, resource allocation. RWS Publications, Pittsburgh. 502 pp.

Saaty, T., 1994. Fundamentals of decision making and priority theory with analytic hierarchy process. RWS Publications, Pittsburgh. 527 pp.

Saaty, T., Vargas, L.G., 2001. Models, methods, concepts, and applications of the analytic hierarchy process. Kluwer Academic, Boston. 333 pp.

Saha, A.K., Gupta, R.P., 2002. GIS-based landslide hazard zonation in the Bhagirathi (Ganga) valley, Himalayas. International Journal of Remote Sensing 23, 357–369.

Saha, A.K., Gupta, R.P., Sarkar, I., Arora, M.K., Csaplovics, E., 2005. An approach for GIS-based statistical landslide susceptibility zonation — with a case study in the Himalayas. Landslides 2, 61–69.

Sarkar, S., Gupta, P.K., 2005. Techniques for landslide hazard zonation; application to Srinagar–Rudraprayag area of Garhwal Himalaya. Journal of the Geological Society of India 65, 217–230.

Schneider, J.-L., Pollet, N., Chapron, E., Wessels, M., Wassmer, P., 2004. Signature of Rhine Valley sturzstrom dam failures in Holocene sediments of Lake Constance, Germany. Sedimentary Geology 169, 75–91.

Sharma, V.K., Kandpal, G.C., 1996. Landslide zonation mapping (LZM); an input for geoenvironmental hazard assessment of a part of Garhwal Himalaya. Special Publication Series, Geological Survey of India 21, 81–84.

Spiker, E.C., Gori, P.L., 2000. National landslide hazards mitigation strategy: a framework for loss reduction. Department of Interior, USGS, Open-file Report 00-450. 49 pp.

Sudmeier-Rieux, K., Qureshi, R.A., Peduzzi, P., Jaboyedoff, M.J., Breguet, A., Dubois, J., Jaubert, R., Cheema, M.A., 2007a. An interdisciplinary approach to understanding landslides and risk management: a case study from earthquake-affected Kashmir. Mountain Forum, Mountain GIS e-Conference, January 14–25, 2008. http://www.mtnforum.org/rs/ec/scfiles/Neelum_PAK_landslides_2007.pdf.

Sudmeier-Rieux, K., Qureshi, R.A., Peduzzi, P., Nessi, J., Breguet, A., Dubois, Jaboyedoff, M., Jaubert, R., Rietbergen, S., Klaus, R., Cheema, M.A., 2007b. Disaster risk, livelihoods and natural barriers, strengthening decision-making tools for disaster risk reduction, a case study from Northern Pakistan. The World Conservation Union (IUCN) Pakistan Programme, Final Report, Karachi. 53 pp.

Swanson, F.J., Dyrness, C.T., 1975. Impact of clearcutting and road construction on soil erosion by landslides in the Western Cascade Range, Oregon. Geology 3, 393–396.

Trommler, N., Huggel, C., Korup, O., Schneider, F.J., 2008. Assessing post-failure geomorphic impact of an earthquake-triggered landslide dam, Jhelum River, Pakistan. Geophysical Research Abstracts 10 EGU2008-A-00622.

USGS (United States Geological Service), 2006. Magnitude 7.6 — Pakistan: earthquake summary. http://earthquake.usgs.gov/eqcenter/eqinthenews/2005/usdyae/#summary accessed 21 August 2007.

Van Westin, C.J., Rengers, N., Soeters, R., 2003. Use of geomorphological information in indirect landslide susceptibility assessment. Natural Hazards 30, 399–419.

Varnes, D.J., 1978. Slope movement types and processes. In: Schuster, R.L., Krizek, R.J. (Eds.), Landslides: analysis and control. National Academy of Sciences, Transportation Research Board Special Report, vol. 76, pp. 12–33.

Varnes, D.J., 1984. Mass-movements landslide hazard zonation: a review of principle and practices. UNESCO Press, Paris. 63 pp.

Vinod Kumar, K., Martha, T.R., Roy, P.S., 2006. Mapping damage in the Jammu and Kashmir caused by the 8 October 2005 M_w 7.3 earthquake from the Cartosat-1 and Resourcesat-1 imagery. International Journal of Remote Sensing 27, 4449–4459.

Virdi, N.S., Sah, M.P., Bartarya, S.K., 1997. Mass wasting its manifestations, causes and control; some case histories from Himachal Himalaya. HIMAVIKAS Occasional Publication 10, 111–130.

Wang, Linlin, Ge, Hua, Xu, Caijun, Du, Zhixing, 2007. 3-D coseismic displacement field of the 2005 Kashmir earthquake inferred from satellite radar imagery. Earth Planets Space 59, 343–349.

WMO (World Meteorological Organization), 2007. Pakistan. http://www.worldweather.org/047/c00901.htm accessed 31 August 2007.

World Gazetteer, 2007. Pakistan: administrative divisions (population and area). http://www.world-gazetteer.com/wg.php?x=&men=gadm&lng=en&dat=32&geo=-172&srt=npan&col=aohdq accessed 31 August 2007.

Yagi, H., 2003. Development of assessment method for landslide hazardness by AHP. Abstract Volume of the 42nd Annual Meeting of the Japan Landslide Society, pp. 209–212.

Yeats, R.S., Parsons, T., Hussain, A., Yuji, Y., 2006. Stress changes with the 8 October 2005 Kashmir earthquake: lessons for future. In: Kausar, A.B., Karim, T., Khan, T. (Eds.), Conference on 8 October 2005 Earthquake in Pakistan: its Implications & Hazard Mitigation, January 18–19, 2006, Islamabad, Extended Abstracts, pp. 16–17.

Zêzere, J.L., Reis, E., Garcia, R.A.C., Oliveira, S.C., Rodrigues, M.L., Vieira, G., Ferreira, A., 2004. Integration of spatial and temporal data for the definition of different landslide hazard scenarios in the area north of Lisbon (Portugal). Natural Hazards and Earth System Sciences 4, 133–146.

Zêzere, J.L., Garcia, R.A.C., Oliveira, S.C., Reis, E., 2008. Probabilistic landslide risk analysis considering direct costs in the area north of Lisbon (Portugal). Geomorphology 94, 467–495.